Large-Angle, Single-Collision Scattering of Argon Ions (40–80 keV) from Metals

SHELDON DATZ* AND CORNELIS SNOEK
FOM—Laboratory for Mass Separation, Amsterdam, The Netherlands
(Received 26 November 1963)

The energy and angular distribution of the "secondary ions" obtained from the bombardment of metallic surfaces (Cu,Ag,Au) by Ar^+ ions (40–80 keV) shows that most of these ions arise from biparticle collisions between the incoming argon ion and a surface atom which is effectively isolated from lattice interactions. Effects attributable to multiple collisions were minimized, in the case of Cu, by the use of oriented single-crystal targets. Multiply charged species of both the projectile atoms (Ar^+ to Ar^{6+}) and the target atoms (1+ to 5+) were detected. Their angular distributions were qualitatively similar to those obtained in previous gas scattering experiments.

INTRODUCTION

STUDIES of large-angle atomic scattering in the 10–100 keV energy region have shown that these collisions are predominantly inelastic and lead to multiple ionizations of the colliding pairs.[1,2] In addition to the intrinsic interest in the physics of these collisions, there also exists a great need for the operational scattering potentials in this energy range for use in problems concerning atomic penetration of solids.[3] These potentials can be derived directly from the angular distribution measurements obtained from scattering experiments.[4] Because of the gas scattering techniques employed, studies have been thus far limited to permanent gas atoms (i.e., hydrogen and the inert gases).

In the present paper a new method is described in which the target atoms are located at the surface of a solid. The success of the method depends upon the assumption that during these collisions the surface atom is effectively isolated from the lattice. This assumption is based upon a consideration of the times and energies involved in such collisions. For ions in the 10–100 keV energy region, these times are in the order of 10^{-16}–10^{-17} sec, whereas vibration times of the target atoms in their lattice are in the order of 10^{-13} to 10^{-14} sec. Thus, when the energy transferred during the collision exceeds the binding energy of the target atom (5–20 eV), one might expect decoupling from lattice interactions.

A number of investigators have observed fast "secondary" ions emitted from ionically bombarded solid surfaces and recent observations have indicated that, in some cases, a measurable fraction of the secondary ions have energies which are characteristic of simple two-atom collisions.[5,6] In the present work, we have employed Ar^+ ion beams with energies ranging from 40 to 80 keV and have investigated the energy and angular distribution of the ions emitted and reflected from polycrystalline Cu, Cu_2O, Ag, and Au, and single crystals of Cu.[7]

EXPERIMENTAL

The Ar^+ ion beam was supplied by a 10–200-keV ion accelerator. This machine, which utilizes a duoplasmatron ion source and a 90° analyzer magnet, furnished a beam of isotopically pure Ar^{40} ions with a current density of $\sim 200\ \mu A/cm^2$. Final collimation of the ion beam was accomplished by a pair of slits at the entrance of the scattering apparatus (see Fig. 1). The maximum divergence angle of the entering beam was 1°. The target was mounted on a holder which could be rotated through an angle ϕ with respect to the incoming beam direction. The target and holder could also be withdrawn from the beam for alignment purposes. The beam current was measured in a Faraday cup which could be inserted immediately in front of the target. The current was monitored during the course of an experiment by directly measuring the target current (uncorrected for secondary electron emission).

The secondary particles entered a momentum analyzer through a pair of 1-mm diaphragms separated by 91 mm, which defined a scattering angle aperture $\Delta\theta$ of $\sim 0.6°$ (Fig. 2). The analyzer consisted of a 60° sector magnet with a radius of curvature of 20 cm. The magnetically analyzed beam entered the detector through a 2-mm slit. The mass and/or energy resolution of the system was thus ~ 100. The detection system consisted of a 17-stage electron multiplier (EMI 9603A), the output of which was read with a General Radio (1230A) electrometer. Because of the effects of stray magnetic fields on the low-energy secondary ions, it was necessary to introduce magnetic shielding wherever possible in the scattering and analyzing region.

The entire secondary analysis system could be rotated about the scattering center through an angle θ, defined with respect to the initial beam direction. This was accomplished by constructing the scattering chamber in

* Guest scientist; permanent address: Oak Ridge National Laboratory, Oak Ridge, Tennessee.

[1] N. V. Fedorenko, Usp. Fiz. Nauk. **68**, 481 (1959) [English transl.: Soviet Phys.—Usp. **2**, 526 (1959)].

[2] G. H. Morgan and E. Everhart, Phys. Rev. **128**, 667 (1962) and references cited therein.

[3] M. T. Robinson and O. S. Oen, Phys. Rev. **132**, 2385 (1963).

[4] G. H. Lane and E. Everhart, Phys. Rev. **120**, 2064 (1960).

[5] V. Walther and H. Hintenberger, Z. Naturforsch. **17a**, 694 (1962).

[6] B. V. Panin, Zh. Eksperim. i Teor. Fiz. **42**, 313 (1962) [English transl.: Soviet Phys.—JETP **15**, 215 (1962)].

[7] A portion of this work concerning polycrystalline targets has appeared in abbreviated form in the Proceedings of the VI International Conference on Ionization Phenomena in Gases, Paris, 1963 (to be published).

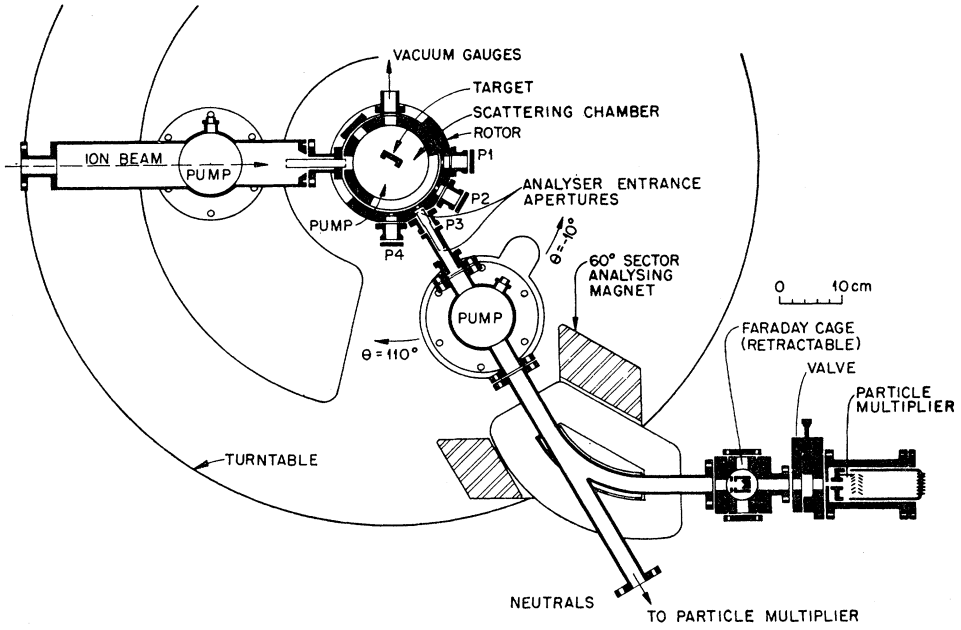

FIG. 1. Plan view of the scattering chamber and momentum analyzer. The rotor could be moved through 35° of arc. The momentum analyzer could be moved through 120° of arc by changing connecting ports (P_1-P_4).

the form of an inverted stopcock as shown in Fig. 1. The closure between the inner and outer members was established with a sliding "O" ring seal. Although the outer member could only be rotated 35° of arc, the analyzer system could be rotated from -10 to $+110°$ by switching the analyzer entrance aperture assembly between the four available entrance ports (marked P_1-P_4).

The system was evacuated with mercury diffusion pumps equipped with liquid air-cooled baffles. Operating pressures in the scattering chamber were in the order of 1×10^{-6} Torr. For many types of experiment

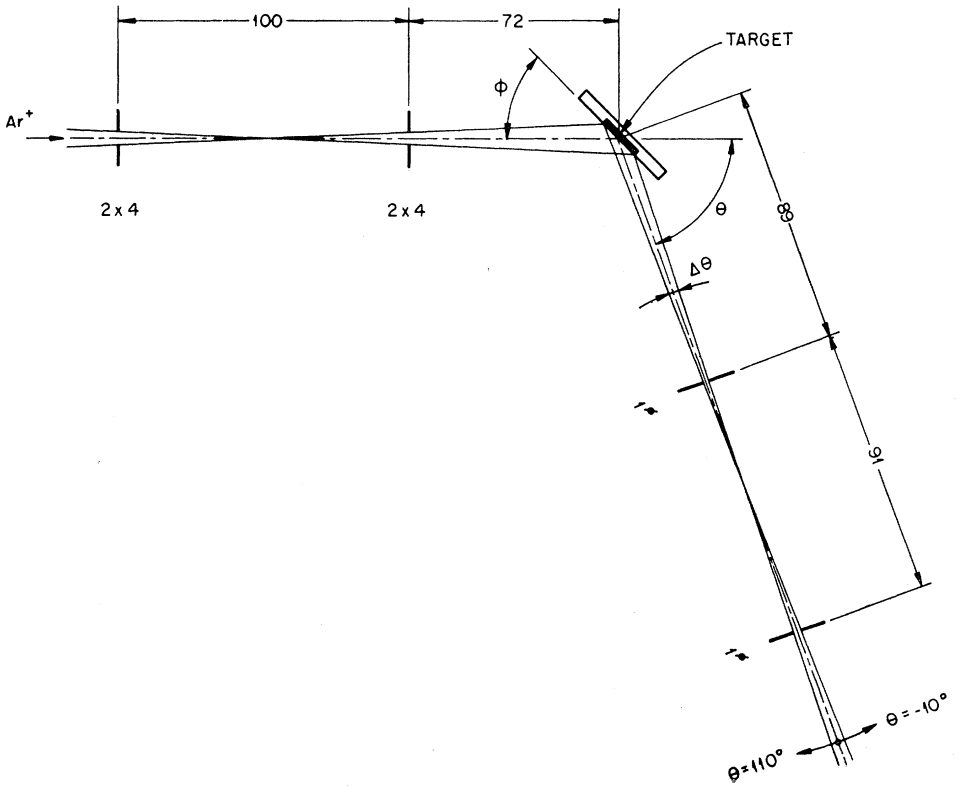

FIG. 2. Schematic representation of the scattering chamber optics. Dimensions are given in mm.

this background pressure would be too high to permit the maintenance of clean surfaces. However, because of the beam current densities employed in this experiment, the cleanliness of the surface was maintained through the rapid removal of surface atoms by sputtering processes; i.e., at a current density of 200 μA/cm^2 the rate at which surface atoms are removed by sputtering ($\sim 10^{16}$ atoms/cm^{2}sec) far exceeds the flux of incoming oxygen molecules from the ambient gas ($\sim 2\times 10^{13}$ molecules/cm^{2}sec). That this was indeed the case, was borne out by the experimental results shown below and by other experiments in which the current density intentionally was lowered to $\sim 10\,\mu$A cm^{-2}. In the latter case other features appeared in the observed spectra which were attributed to adsorbed impurities.

RESULTS AND DISCUSSION

The target was placed at a fixed angle ϕ with respect to the incoming beam, the analyzer was rotated to a fixed angle θ and the ion current I into the detector was measured as a function of the magnetic field B. Typical plots of I versus B are given in Fig. 3 for Ar$^+$ ions incident on polycrystalline Cu, Ag, and Au. It can be seen that the spectra consisted of a series of relatively sharp lines superimposed on a low background. The peak heights, in some cases, were about a hundred times larger than the background current levels.

In order to understand the assignment of these lines to the various ionic species it is necessary to consider the behavior which would be expected if the ion beam were directed at a stationary-gas atom target. In this case the energies of the scattered particles are uniquely determined by the scattering angle.[8] The maximum energy E_m, which could be transferred from a projectile atom of mass M_1 with an initial kinetic energy E_0 to a target atom of mass M_2, is given by

$$E_m=[4M_1M_2/(M_1+M_2)^2]E_0. \quad (1)$$

The actual energy transferred to the target particles E_2 in a collision, is related to the scattering angle θ:

$$E_2=E_m\cos^2\theta. \quad (2)$$

The energy of the projectile particle scattered into the angle θ is given by

$$E_1=E_0(1+\alpha)^{-2}[\cos\theta\pm(\alpha^2-\sin^2\theta)^{1/2}]^2, \quad (3)$$

where $\alpha=M_2/M_1$. The condition for focusing in the magnetic analyzer is

$$B=k(EM)^{1/2}/Z, \quad (4)$$

where Z is the ionic charge and k is the spectrometer constant (for the instrument used, $k=6.3$).

Thus, for a two-particle collision, the value of $M^{1/2}/Z$ for the ion collected may be determined from B, since E is known for a given E_0 and θ.

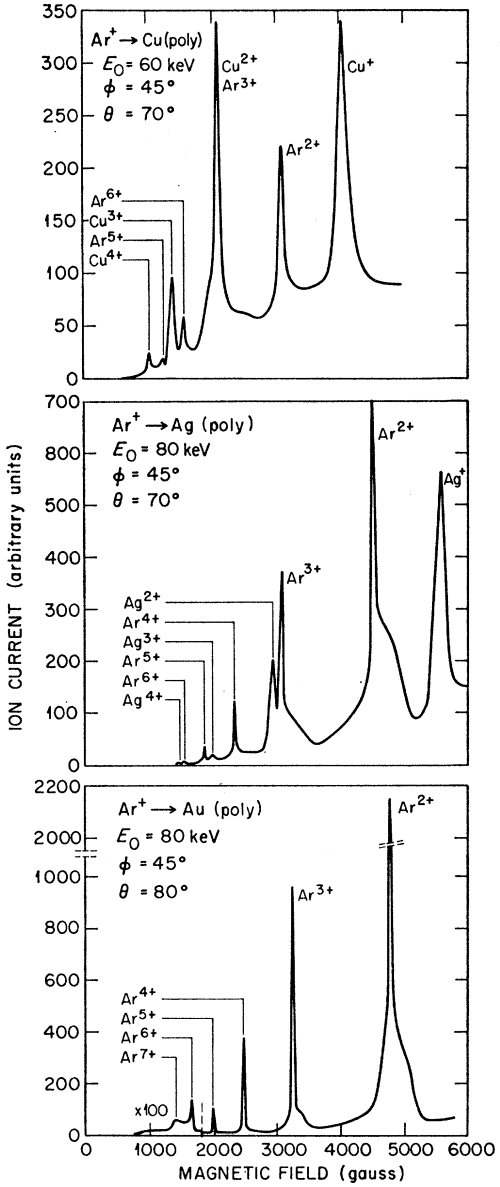

FIG. 3. Magnetic analysis of the scattered ion currents for the systems Ar$^+$ (60 keV) on Cu ($\theta=70°$), Ar$^+$ (80 keV) on Ag ($\theta=70°$) and Ar$^+$ (80 keV) on Au ($\theta=80°$). The targets in these cases were all polycrystalline.

If it is assumed that the peaks in the spectra recorded in Fig. 3 correspond to ions which have been scattered by single two-atom collision (i.e., isolated from the lattice), the ionic species may readily be identified from Eq. (4). Since we also know $(\partial E/\partial\theta)$ [cf. Eqs. (2) and (3)] the validity of this assumption can be tested without a direct measurement of the ion energy by measuring the angular dependence of the B value corresponding to a given peak. Observations were made with initial energies of 40, 60, and 80 keV in the angular region from

[8] This is strictly true only for totally elastic collisions, but if inelastic energy loss is small compared to the kinetic energy of the particles, only small deviation should occur.

$\theta=60$ to $\theta=110°$, and were in complete accord with the two-body assumption. Also in accord with the biparticle-collision mechanism was the observation that, in the case of the polycrystalline samples, the spectrum was not altered when the surface incidence angle ϕ was varied.

In the cases of Cu and Ag, sets of peaks were observed which could be attributed to charged states of projectile particles (Ar^+ to Ar^{6+}), which had been reflected from metal target atoms and to ejected target atoms (Cu^+ to Cu^{5+} and Ag^+ to Ag^{4+}). The peak sets could easily be differentiated by the stronger angular dependence of the target ion energies and by the complete disappearance of target ion peaks at scattering angles above 90°. In the case of Au, only the scattered projectile ions could be detected (Ar^+ to Ar^{7+}), the mass of the Au ions being too high to be detected in our available range of B. In no case were any peaks observed which could be attributed to the scattering of Ar ions from Ar atoms in the target.

The peak widths for the single collision events are determined by the angular acceptance aperture of the analyzer and the species observed. With a given angular aperture $\Delta\theta$, the energy spread in the scattered projectile particles is

$$\Delta E_1/E_1=2\Delta\theta\sin\theta(\alpha^2-\sin^2\theta)^{-1/2}. \quad (5)$$

Similarly, for the target particles

$$\Delta E_2/E_2=2\Delta\theta\tan\theta. \quad (6)$$

For all the cases reported, these relationships predict

$$(\Delta E_2/E_2)>(\Delta E_1/E_1).$$

In the case of copper and silver, additional broadening is introduced by the presence of two abundant isotopes in the target, i.e., Cu^{63}(68%), Cu^{65}(32%), and Ag^{107}(53%), Ag^{109}(41%). This gives rise to two separate scattering spectra corresponding, e.g., to the $Ar^{40}-Cu^{63}$ and $Ar^{40}-Cu^{65}$ systems. The differences in the angular dependence of the energy for the two systems can be seen in Fig. 4. These spectra are not resolved in the case of polycrystalline targets because of effects attributable to multiple-scattering events.

The contribution of multiple collision events to the observed spectrum can be seen most clearly in the argon peaks reflected from Au and Ag, where shoulders appear on the high-energy flanks of the peaks. This effect may be understood by comparing the energy of a projectile particle scattered into a given angle θ_1 by a single collision with that of a similar particle which has been scattered into the same angle by a sequence of two or more collisions. It will be unlikely that a multiple collision sequence will involve a scattering angle greater than θ_1, since the magnitude of the scattering cross section decreases with increasing scattering angle. Thus, most of the multiply scattered particles observed will have undergone collisions, each of which involves a smaller scattering angle. From Eq. (3) it can be shown that the final energy of these particles will be higher than the energy of those which have been scattered into the same angle by a single collision (e.g., for an Ar ion scattered from a Cu atom into $\theta=70°$ by a single collision $E_1=0.4E_0$, whereas one which is scattered into the same angle by a sequence of two 35° deflections would have $E_1=0.64E_0$).

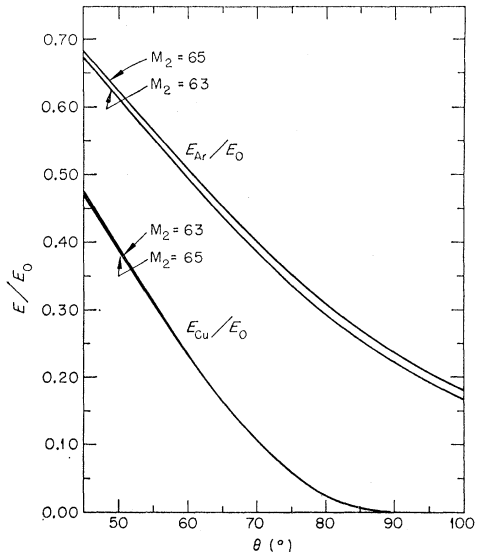

FIG. 4. The fraction of the initial ion energy E_0 possessed by a scattered particle as a function of the laboratory angle θ for the atomic scattering of Ar from Cu. The upper two curves represent the energy of an Ar^{40} particle which has been scattered from a Cu^{65} or a Cu^{63} particle, respectively, while the lower two represent the energy gained by a Cu^{63} or Cu^{65} in the collision.

A further observation of interest is that the relative contribution of multiple collisions to the spectrum decreases with increasing ionic charge. This is most easily seen in the case of the Au target [Fig. 3(c)], where there is no interference from target ions. Two arguments may be proposed to explain this phenomenon. The first is that the multiply scattered particles have undergone less violent collisions and the second is that, even if the

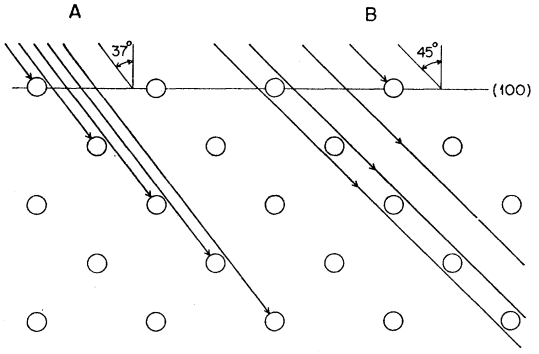

FIG. 5. An illustration of the shadowing effect of surface atoms in the bombardment of a fcc crystal in a [110] direction.

projectile is highly ionized by its first encounter, it will have a chance of picking up electrons from its second collision partner.

The probability that a reflected projectile particle will have made more than one collision with lattice atoms is strongly dependent on the depth of its first collision partner; i.e., an entering particle making its first collision in the third or fourth lattice layer has a much greater chance of making other collisions before leaving the lattice than one which has made its first collision in the first lattice layer. However, the probability of escape from the lattice decreases with increasing initial penetration depth. Thus, the contribution of multiple collision events to the spectrum could be greatly reduced by arranging the target so that the projectile either makes its first collision in the first atomic layer or that it penetrates so deeply into the lattice before colliding that its ultimate emergence becomes highly improbable.

This condition was achieved experimentally by directing the beam at a (100) copper single crystal which had been rotated 45° about another [100] axis in the surface. With this configuration (see rays marked B in Fig. 5) the argon ions enter the crystal in a [110] direction in which all atoms lying below the top layer are shielded by surface atoms. Ion spectra observed using this arrangement are shown in Fig. 6 for three different detection angles ($\theta=70$, 80, and 90°). Several interesting properties can be correlated with the predictions of Fig. 4:

1. The large angular energy dependence of the Cu spectrum; 2. the disappearance of target species at $\theta=90°$ corresponding to $E_2=0$; 3. the much decreased "background" spectrum (as compared with Fig. 3A); 4. the splitting of all the argon lines into doublets corresponding to scattering from Cu^{63} and Cu^{65}; 5. the correspondence of the peak-height ratios in the doublets to the Cu isotopic-abundance ratio (~2:1); 6. the width and lack of mass resolution in the Cu-ion peaks, due, primarily, to the large $\Delta E/\Delta\theta$ for this species in this angular region.

In order further to ascertain that the differences between the spectra obtained from polycrystal and oriented single-crystal targets were indeed the result of shadowing by the first atomic layer, spectra were obtained with the same crystal rotated to an angle $\phi=37°$. At this incidence angle the incoming particle can make its first collision several atom layers down from the surface. (Rays marked A in Fig. 5.) The differences observed are typified in Fig. 7 where the multiple collision broadening is seen to erase the resolution obtained in the case of 45° incidence.

Angular Distributions

The nature of the target surface limits the angular region in which quantitative observations can be made. If the solid were perfectly planar and atomically smooth, one could make measurements at very low values of θ by using a small value of ϕ (grazing incidence). The sputtering process, however, will create surface ridges even on a previously planar target and these ridges will intercept some of the particles emanating from the valleys on the surface. The maximum useable angle is thus obtained when the surface ridges make the minimum angle with the original surface plane.

In an earlier optical study on the configuration of the surface irregularities created on a (100) Cu crystal face

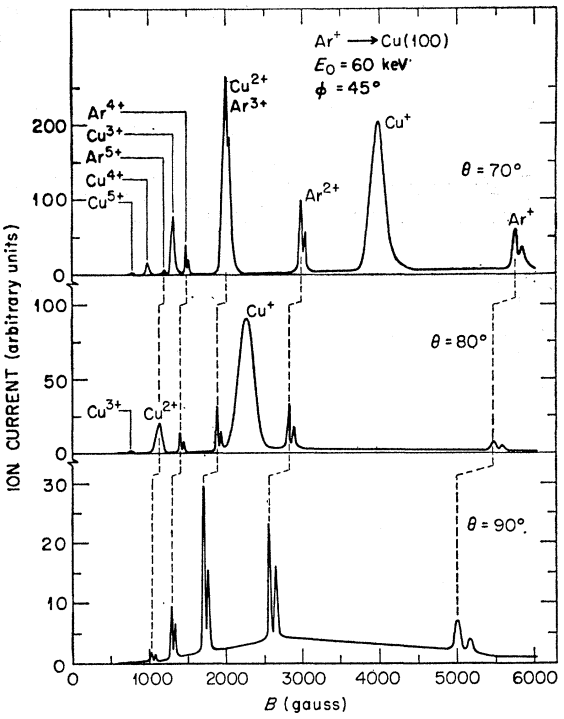

FIG. 6. Magnetic analysis of the scattered ion currents obtained at $\theta=70$, 80, and 90° from the bombardment of a Cu single crystal by 60-keV Ar^+. In this case the ion beam entered the crystal in a [110] direction.

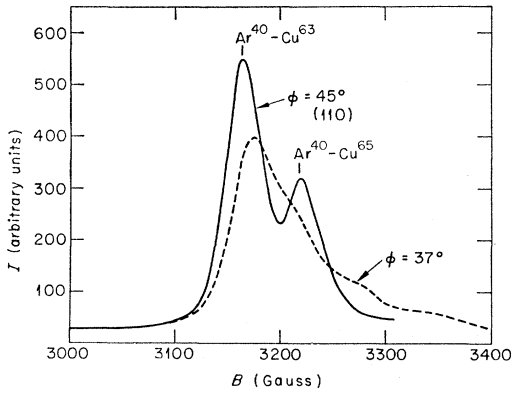

FIG. 7. Line shape of the Ar^{2+} peak ($E_0=60$ keV, $\theta=70°$) reflected from a (100) Cu crystal for ion beam incidence at $\phi=45°$ [110], and at $\phi=37°$.

by Ar-ion bombardment[9] it had been observed that the ridges formed by bombardment along a [110] axis ($\phi=45°$) had a considerably smaller pitch ($\sim 15°$) than those created by bombardment along a high-index direction (e.g., for $\theta=37°$ the pitch was 45° to the surface). Therefore bombardment of a (100) crystal face along a [110] axis has the advantage not only of minimizing the contribution of multiple collisions to the spectra but also of minimizing the effect of surface irregularities.[10] This experimental configuration thus permitted observation in the angular region $60°<\theta<110°$, the upper limit being set by the limit of rotation of the detector. This range corresponds to center-of-mass angle scattering of the target Cu atoms of from $\psi=0$ to 60° and for the projectile Ar atoms $\psi=90$–145°. It should be noted that although partial shadowing by surface irregularities can introduce a major error in the total differential cross sections, the effect should not interfere with the determination of the relative partial differential cross sections (i.e., the fraction of ions in a given charge state at a given angle).

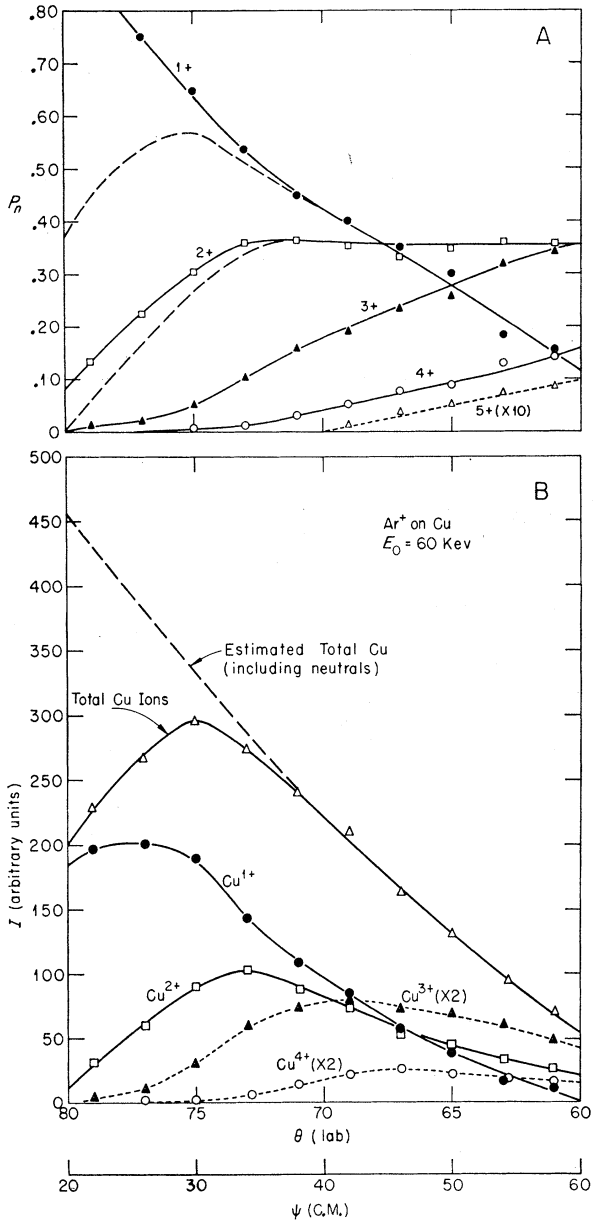

FIG. 8. Angular distribution of the Cu ion species, for Ar^+ (60 keV) on Cu. The relative probabilities are plotted in the upper portion (A) and the ion currents are plotted in (B). The dashed extrapolations in A refer to the assumption of a neutral component as indicated in (B).

[9] J. M. Fluit and S. Datz, Physica (to be published).

Some of the angular distributions observed for $E_0=60$ keV are shown in Figs. 8 and 9. A calculation of the distance of closest approach in the given angular intervals based upon the assumption of a shielded Coulomb potential and utilizing the curves given by Lane and

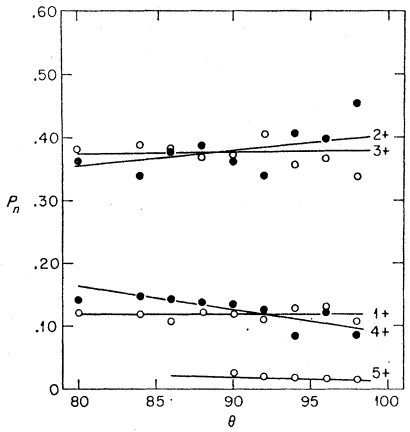

FIG. 9. Angular distribution of the relative probabilities of the Ar ion species for Ar^+ (60 keV) on Cu in the angular region $\theta=80-100°$.

Everhart[4] indicates that the distance of closest approach corresponding to this degree of scattering varies at $E_0=60$ keV from 0.22Å at $\theta=80°$ to 0.12 at $\theta=60°$ for Cu and from 0.105Å at $\theta=80°$ to 0.098Å at $\theta=100°$ for Ar.

In Fig. 8(B) we have plotted the angular distribution of the Cu ion intensities and the sum of the various ion intensities. For bombarding energies of 40 and 80 keV similar curves were obtained. With increasing E_0 the positions of the peaks were shifted toward lower center-of-mass angles. It is interesting to note, however, that the peaks for a given ionic species occurred at about the same value of E_1, the transferred energy, independent of E_0.

Since any reasonable model of a scattering potential

[10] Because optical methods were used in the quoted work, irregularities observed were only those which were larger than the wavelength of the light used. The existence of smaller irregularities with a higher pitch would further disturb the distribution measurements.

would predict a monotonic rise in the total differential cross section, the decline of the total ion current above $\theta=75°$ implies that, with decreasing energy transfer, an increasing fraction of the copper is leaving the crystal as neutral atoms. That an appreciable amount of the Cu fast atoms leave the surface as excited neutrals has already been established by previous work from this laboratory[11,12] in which the line spectrum of Cu *I* was observed from Cu bombarded by 20-keV Ar^+.

Several attempts were made to measure the neutral atom component by detecting with an electron multiplier the fast particles which had not been deflected by the magnetic field. However, these measurements were inconclusive because of the presence of a large photon background. Thus, the dashed curve in Fig. 8(B) is based completely on an assumption of negligible neutral atom contribution below $\theta=70°$.

In Fig. 8(A) and 9 we have plotted the angular dependence of the relative probabilities for the various ion species. In addition to compensating for the change in total cross section with angle, this type of plot also compensates for possible differences in collection geometry due either to misalignment or partial shadowing by surface projections. For comparison, Fig. 10 shows the data obtained by Fuls *et al.*[13] for the scattering of 50-keV Ar^+ from Ar in the angular region $\theta=0$ to 40° (ψ from 0–80°). Thus, in terms of distance of closest approach and energy exchange, the data shown for the Cu ion species in the region $\theta=60$–80° should correspond roughly to the left-hand region of Fig. 10 while the data shown for the reflected Ar species in Fig. 9 correspond to an extrapolation of the right-hand side of Fig. 10.

Two similarities are immediately obvious. First is the rapid rise and fall of the relative probabilities of formation of the Cu ions in their various charge states and second is the relative constancy of the Ar-ion charge-state probabilities at large scattering angles. This latter effect is to be expected since at the larger scattering angles the distance of closest approach varies only slightly with angle because of the steepness of the potential in this region.

The major over-all differences are in the relative probabilities of the higher charge states. The results of present work indicate lower probabilities for higher charge states than were obtained in the Ar^+—Ar system. The ionization probabilities are clearly connected with the electronic structure of the reactant species and the observed differences may indeed reflect the physical differences between an Ar^+ ion striking an Ar atom with $3p^6$ outer-shell configuration and an Ar^+ ion striking a

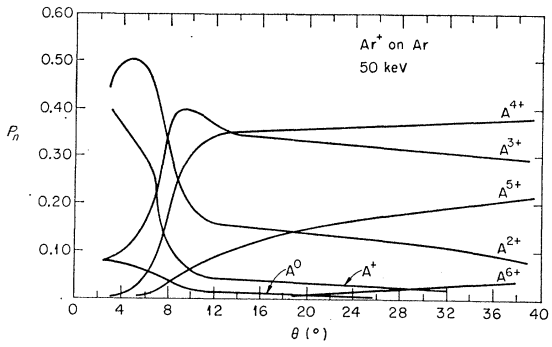

FIG. 10. Angular distribution of the relative probabilities of the Ar ion species for Ar^+ (50 keV) on Ar. From the paper by Fuls *et al.* (see Ref. 13 in text).

Cu^+ ion with a $3d^{10}$ configuration.[14] The only absolute test of the equivalence of ion-surface atom collisions to true gas collisions would be to study the same atomic systems by both techniques. However, in lieu of this information and because of the novelty of the method used we have investigated a number of the possibilities which might lead to spurious interpretation of the results.

One feature which might be expected to perturb the ion scattering spectrum obtained from surface atoms in this way is the presence of conduction electrons in the metal crystal. One might expect a high probability of ion neutralization (or partial neutralization) by electron capture from the "Fermi sea" as the ion is leaving the surface.[15] Although it is not possible to predict the relative probabilities of electron capture for the different charge states of the ions, it would be expected that these probabilities would be different from each other.

In order to assess the importance of this effect, a comparison was made between a polycrystalline Cu target and a Cu_2O target. (The Cu_2O target was prepared by heating Cu to ~1000°C in air for several hours. The resulting oxide layer was ~0.5-mm thick. The resistance between two probes placed 1 mm apart on the surface was $10^5\ \Omega$. This conductivity was enough to prevent distortion of the ion beam by surface charge buildup.) In the case of Cu_20, the Cu also exists as a singly charged ion but the conduction band is substantially vacant and the valence band lies ~1 eV below the conduction band. If electron capture were a serious perturbation on the ion spectra, significant differences in the spectra might be expected. The results shown in Fig. 11 indicate that this was not the case. Although the general background level was higher with the Cu_2O target, the ratio of the relative peak heights (e.g., Cu^+/Cu^{4+}) was the same as that obtained from metallic Cu. (Peaks corresponding to the scattering of argon from oxygen atoms should not be observed since the maximum scattering angle for this system is $\theta=23°$.) It might also be

[11] J. Kistemaker and C. Snoek in *Le Bombardement Ionique* (Editions du Centre National de la Recherche Scientifique, Paris, 1962).
[12] C. Snoek, W. F. van der Weg, and P. K. Rol, Physica (to be published).
[13] E. N. Fuls, P. R. Jones, F. P. Ziemba, and E. Everhart, Phys. Rev. **107**, 704 (1957).
[14] We are assuming here that at the surface of the metal the copper exists as a singly charged ion.
[15] H. D. Hagstrum, Phys. Rev. **123**, 758 (1961).

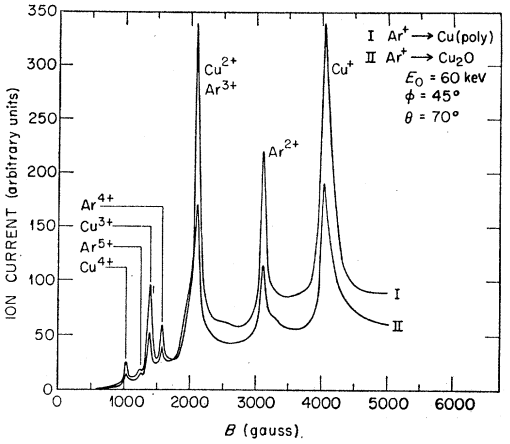

FIG. 11. Magnetic analysis of the scattered ion currents obtained at $\theta=70°$ from 60-keV Ar^+ bombardment of polycrystalline Cu (curve I) and Cu_2O (curve II).

argued that the probability of charge transfer neutralization from the metal would become more important as the velocity of the Cu particle leaving it was decreased. From this argument it would be expected that the angular peak of Cu^+ ion distribution would be shifted towards 90° but a measurement of the angular distribution of Cu^+ from Cu_2O gave identical results to that obtained for Cu metal. Thus, within the limits of these tests, it appears that conduction electrons do not seriously perturb the ion spectra.

Because the observed differences could also clearly be due to a host of apparatus effects, an experiment described by Fuls *et al.*[13] was redone in our apparatus. This was accomplished simply by removing the solid target, filling the scattering chamber with argon gas to a pressure of $\sim 1\times10^{-4}$ Torr, and bombarding with a 50 keV Ar^+ beam. The results obtained were in good accord with the previous work (see Fig. 10). A particularly sensitive test was the observation of the crossover of the relative probabilities for the formation of Ar^+ and Ar^{5+}, and the $Ar^{2+}-Ar^{4+}$ at $\theta=11°$.

The agreement in results eliminated the possibility of many, but not all, apparatus effects. Thus, although the copper ions have undergone collisions comparable in violence with the Ar ions in the low-angle region of Fig. 11, the kinetic energies of the copper ions (0–6 keV) are considerably less than those of their counterparts in the gas scattering experiment. Therefore, the effects of stray magnetic fields, and of electric fields from the collection of charge on imperfectly cleaned surfaces, could have a more serious effect on the measurement of the Cu ions. Moreover, since these effects would be larger the larger the ionic charge, their presence could give spuriously low values for the relative probabilities of more highly charged ions. Attempts were made to correct this possible instrumental fault by rigorous cleaning of the apparatus, the use of gold apertures, and the application of "alquadag"[16] to the inner surfaces of the apparatus. But these changes caused no significant changes in the results.

Another possible process which could cause preferential loss of low-velocity, highly charged ions is that of charge exchange with the residual gas in the apparatus. To test this hypothesis the ambient pressure of 1×10^{-6} in the scattering chamber was intentionally raised by a factor of 10 by the admission of Ar gas. But no changes were observed in the spectra.

Within the limits of the test mentioned above, the results seem to represent a real physical situation. However, although the shapes of the individual ion curves and the angular positions of their maxima were quite reproducible, some indeterminate changes in the experimental system did cause variations in the observed relative intensities of the ion species. We have therefore not attempted any quantitative evaluation of the absolute cross sections in this paper.

Conclusions

It has been established that the dynamical behavior of the ions emitted and reflected from metallic surfaces subjected to argon ion bombardment ($E_0=40$–80 keV) can be exactly described on the basis of biparticle collisions between incoming ions and surface atoms which are effectively isolated from lattice interactions. The existence of multiply charged ions of both the target and projectile species was established. The angular dependence of the relative differential scattering cross sections for the various charged species was measured and found to be qualitatively similar to the observation of previous workers on gas targets.

Signals arising from multiple collision events are reduced to inappreciable levels when single crystals with the proper orientation are used for targets and perturbation of the ionic charge distributions by conduction electrons in the metal does not seem to be important.

The use of a solid target technique for large-angle atomic scattering studies potentially possesses two advantages over gas scattering methods. First is the increase in the number and type of target atoms which may be used and second is the increase in target atom density which yields an equal increase in signal and attainable angular resolution. In the region of $\theta=60$–$110°$, not only were target ions observed but also projectile ions which had undergone very large angle scattering. Therefore in this case the center-of-mass angular region which can be studied extends from 0 to almost 150°.

ACKNOWLEDGMENTS

The authors with to thank Professor J. Kistemaker for his stimulating interest in this work, and E. de Haas for the construction of the apparatus. It is a pleasure to

[16] E. Lindholm, Rev. Sci. Instr. 31, 210 (1960).

acknowledge S. Doorn and F. Steenbergen for their aid in carrying out the experiments and J. M. Fluit, P. K. Rol, and J. Sanders for many useful discussions.

This work is part of the Research Program of the Stichting voor Fundamenteel Onderzoek der Materie, and was made possible by financial support from the Nederlandse Organisatie voor Zuiver Wetenschappelijk Onderzoek.

PHYSICAL REVIEW VOLUME 134, NUMBER 2A 20 APRIL 1964

Mobility of Electrons in the Noble Gases*

JOSEPH C. BOWE
Radiological Physics Division, Argonne National Laboratory, Argonne, Illinois
(Received 28 October 1963)

This paper presents a theoretical study which leads to formulas that relate the cross section for inelastic collisions near the threshold energy to the drift velocity v_d of electrons in noble gases. Derivation of general formulas for v_d follows a qualitative interpretation of the main features of the experimental drift-velocity curves. The formulas for v_d are derived for the case in which the elastic cross section for momentum transfer is given by $N_0Q_m(v)=av^{i-1}$. Closed-form expressions for v_d are obtained by integrating only over the distribution function for electrons that have energy less than the excitation energy u_1. By this procedure, integration over the high-energy ($u>u_1$) distribution function is avoided and the use of analytical methods is made possible. A partial correction to this approximation is obtained by extending the low-energy ($u<u_1$) distribution function to pass through zero at an energy u_0 that is greater than u_1. From the drift-velocity formula and the experimental values of v_d, the cutoff energy u_0 can, in principle, be evaluated as a function of E/p. The high-energy distribution function is used to derive an expression for the overshoot (u_0-u_1) which is shown to be proportional to $(E/p)^{2/(\gamma+2)}$ and to depend upon the constants h and γ when the inelastic-collision cross section has the form $Q_1(u)=h(u-u_1)^\gamma$. Possible applications of these theoretical results to drift-velocity data for gas mixtures are also briefly discussed.

I. INTRODUCTION

THE drift velocity of electrons in the noble gases has a remarkably simple dependence (Fig. 1) upon E/p (the ratio of applied field to gas pressure) that bears a direct relation to the fundamental collision processes between electrons and gas atoms. It is therefore of interest to show how these characteristics of the drift-velocity data peculiar to the noble gases can be understood from theory. In particular, it is desired to obtain a better understanding of the effect that inelastic collisions have upon the drift velocity. The striking up-turn in the drift-velocity curve is assumed to be closely correlated to the cross section for inelastic collision. By making a more thorough study of the role of inelastic collisions than was made in earlier publications,[1] this paper derives formulas in closed form by which the cross section for excitation near threshold can, in principle, be deduced from drift-velocity data. The present paper adds to and extends the previously published work by obtaining formulas for the drift velocity in terms of a cutoff energy u_0 and by finding a relation between u_0 and the cross section for inelastic collisions.

The drift velocity of a swarm is a macroscopic quantity, whereas the collision cross section is an atomic quantity. The macroscopic properties, however, are determined by the atomic properties and the interdependence of the two is formulated by statistical theory in which the Maxwell-Boltzmann transport equation defines the velocity distribution for electrons. Analytical formulas that relate the drift velocity to the atomic cross section for elastic collisions have indeed already been derived for the region of low E/p where inelastic collisions are neglected.[2] For the region of

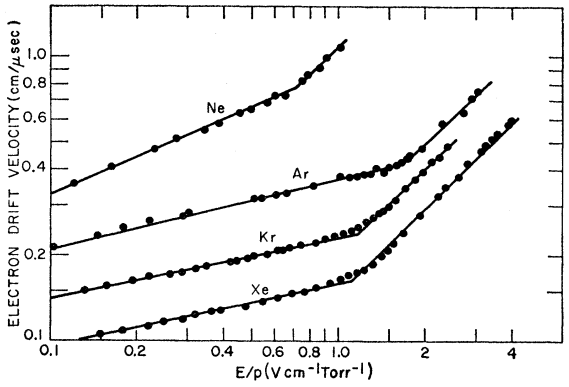

FIG. 1. Experimental drift-velocity curves for electrons. Inelastic collisions cause the slope to abruptly assume the value unity at $(E/p)^*$. Data for helium are not shown because the break in this curve is partly due to the decreasing cross section for elastic collisions above a few eV. (Notice that the plot is on a log-log scale.)

* Work performed under the auspices of the U. S. Atomic Energy Commission.

[1] P. Walsh, Bull. Am. Phys. Soc. **7**, 632 (1962); D. Barbiere, Phys. Rev. **84**, 653 (1951); H. W. Allen, *ibid.* **52**, 707 (1937); M. J. Druyvesteyn, Physica **4**, 464 (1937).

[2] J. C. Bowe, Phys. Rev. **117**, 1416 (1960).